Application of higher-order structural theory to bending and free vibration analysis of sandwich plates with CNT reinforced composite facesheets

Sundararajan Natarajan[a,1], Mohamed Haboussi[b], Manickam Ganapathi[c]

[a] *School of Civil and Environmental Engineering, The University of New South Wales, Sydney, NSW 2052, Australia.*
[b] *Université Paris 13-CNRS, LSPM, UPR 3407, Villetaneuse, F-93430, France.*
[c] *Tech Mahindra Ltd., Electronic City, Bangalore-560100, India.*

arXiv:1403.1712v1 [math.NA] 7 Mar 2014

Abstract

In this paper, the bending and free flexural vibration behaviour of sandwich plates with carbon nanotube (CNT) reinforced facesheets are investigated using QUAD-8 shear flexible element developed based on higher-order structural theory. This theory accounts for the realistic variation of the displacements through the thickness, and the possible discontinuity in slope at the interface, and the thickness stretch affecting the transverse deflection. The in-plane and rotary inertia terms are considered in the formulation. The governing equations obtained using Lagrange's equation of motions are solved for static and dynamic analyses considering a sandwich plate with homogeneous core and CNT reinforced face sheets. The accuracy of the present formulation is tested considering the problems for which solutions are available. A detailed numerical study is carried out based on various higher-order models deduced from the present theory to examine the influence of the volume fraction of the CNT, core-to-face sheet thickness and the plate thickness ratio on the global/local response of different sandwich plates.

Keywords: Carbon nanotube reinforcement, sandwich plate higher-order theory, mechanical loading, thermal loading, free vibration, shear flexible element.

1. Introduction

Engineered materials, mostly inspired from nature have been replacing the conventional materials due to their high strength-to- and stiffness-to-weight ratios. Among the various structural constructions, the sandwich type of structures are more attractive due to its outstanding bending rigidity, low specific weight, excellent vibration characteristics and good fatigue properties. These sandwich constructions can be considered for the requirement of light weight and high bending stiffness in design by appropriate choice of materials. The response of such structures depends on the bonding characteristics. A typical sandwich structure may consist of a homogeneous core with face sheets. To improve the characteristics, the face sheets can be laminated composites [1], functionally graded materials [2] or polymer matrix with reinforcements [3]. Recent introduction of carbon nanotubes (CNTs) as reinforcement has attracted researchers to investigate the responses of such structures [4]. Experimental investigations show that the CNTs have extraordinary mechanical properties than those of carbon fibers [5]. The CNTs are seen as promising reinforcement for sandwich face sheets. Thostenson and Chou [6] showed that the addition of nanotubes increases the tensile modulus, yield strength and ultimate strengths of the polymer films. Their study has also showed that the polymer films with aligned nanotubes as reinforcements yield superior strength to randomly oriented nanotubes. The properties of the polymer films can also be optimized by varying the distribution of CNTs through the thickness of the film. Moreover, Formica *et al.,* [7] highlighted that the CNT reinforced plates can be be tailored to respond to an external excitation. This has generated interest among researchers. For predicting the realistic behaviour of sandwich structures, more accurate analytical/numerical models based on the three-dimensional models may be computationally involved and expensive. Hence, among the researchers, there is a growing appreciation of the importance of applying two-dimensional theories with new kinematics for

[1] School of Civil and Environmental Engineering, The University of New South Wales, Sydney, NSW 2052, Australia. Tel: +61 293855030; E-mail: s.natarajan@unsw.edu.au; snatarajan@cardiffalumni.org.uk

the evolution of the accurate structural analysis. Various structural theories proposed for the laminated structures have been examined and some of the important contributions pertaining to the sandwich laminated plates are discussed here.

Based on the first-order shear deformation theory, Zhu *et al.,* [8] studied the static and free vibration of CNT reinforced plates. They considered polymer matrix with CNT reinforcement, neglecting the temperature effects. It was predicted that the CNT volume fraction has greater influence on the fundamental frequency and the maximum center deflection. Wang and Shen [9] studied the large amplitude vibration of nanocomposite plates resting on elastic foundation using a perturbation technique. The governing equations were based on higher-order shear deformation theory and the composite plates were reinforced with carbon nanotubes. Their study brought out that while the linear frequencies decrease with the addition of CNTs, the nonlinear to linear frequency ratio increased, especially when increasing the temperature or by decreasing the foundation stiffness. Arani *et al.,* [10], Liew *et al.,* [11] and Lei *et al.,* [12] studied the buckling and post-buckling characteristics of CNT reinforced plates using the finite element method and meshless methods, respectively. It was shown that the reinforcement with CNT increasing the load carrying capacity of the plate. Aragh *et al.,* [13] used generalized differential quadrature and obtained a semi-analytical solution for 3D vibration of cylindrical panels. It was shown that graded CNTs with symmetric distribution through the thickness have high capabilities to alter the natural frequencies when compared to the uniformly distributed or asymmetrically distributed.

It is observed from these investigations that first- order shear deformation theory has been widely employed by many researchers whereas higher-order model considering variation in in-plane displacements has been used by few authors for the analysis of CNT reinforced plates. However, the available literature pertaining to sandwich structures with CNT reinforced face sheets is rather limited compared to plates. Also, to the authors knowledge, the theories accounting the variation of in-plane displacement through the thickness, and the possible discontinuity in slope at the interface, and the thickness stretch affecting transverse deflection is not exploited while investigating the structural behavior of CNT reinforced sandwich structures. A layerwise theory is the possible candidature for this purpose, but it may be computationally expensive as the number of unknowns to be solved increases with increase in the number of mathematical or physical layers. Ali *et al.,* [14] and Ganapathi and Makhecha [15] have used an alternative higher-order plate theory based on global approach, for multi-layered laminated composites by incorporating the realistic through the thickness approximations of the in-plane and transverse displacements by adding a zig-zag function and higher-order terms, respectively. This formulation has proved to give very accurate results for the composite laminates. Such a model for the current problems is considered while comparing with the other approaches available in the literature

Approach. In this paper, a $\mathcal{C}^o$ 8-noded quadrilateral plate element with 13 degrees of freedom per node [15, 16, 17] based on higher order theory [14] is employed to study the static deflection and free vibration analysis of thick/thin sandwich carbon nanotube reinforced functionally graded material plates. The efficacy of the present formulation, for the static analyses subjected to mechanical and thermal loads, and the free vibration study is illustrated through the numerical studies by employing various structural models deduced from the present higher-order accurate theory.

Outline. The paper is organized as follows. The computation of the effective properties of carbon nanotube reinforced composites are discussed in the next section. Section §3 presents the higher order accurate theory to describe the plate kinematics and Section §4 describes the 8-noded quadrilateral plate element employed in this study. The numerical results for the static deflection and the free vibration of thick/thin sandwich carbon nanotube reinforced functionally graded plates are given in Section §5, followed by concluding remarks in the last section.

2. Theoretical Formulation

Consider a rectangular sandwich plate with co-ordinates x and y along the in-plane directons and z along the thickness direction as shown in Figure 1. The core-to-facesheet thickness ratio is h_H/h_f, where, h_H is the core thickness and h_f is the facesheet thickness. The length, the width and the total thickness of the plate are a, b and

h (see Figure 1). A Cartesian coordinate system is assumed and the origin is located at the corner of the plate on the middle plane. We assume that the CNT reinforced layer is made from a mixture of single walled CNT, graded distribution in the thickness direction and the matrix is assumed to be isotropic. The effective properties of such reinforced structures can be computed by Mori-Tanaka scheme [13] or by the rule of mixtures. In this study, we employ simple rule of mixtures with correction factors to estimate the effective material properties of CNT reinforced matrix. The effective material properties of the CNT reinforced matrix are given by [18]:

$$\begin{aligned} E_{11} &= \eta_1 V_{\mathrm{CN}} E_{11}^{\mathrm{CN}} + V_m E_m \\ \frac{\eta_2}{E_{22}} &= \frac{V_{\mathrm{CN}}}{E_{22}^{\mathrm{CN}}} + \frac{V_m}{E_m} \\ \frac{\eta_3}{G_{12}} &= \frac{V_{\mathrm{CN}}}{G_{12}^{\mathrm{CN}}} + \frac{V_m}{G_m} \\ \nu_{12}^{\mathrm{CN}} &= \nu_{12}^{\mathrm{CN}} V_{\mathrm{CN}}^* + \nu_m V_m \\ \rho &= \rho_{\mathrm{CN}} V_{\mathrm{CN}} + \rho_m V_m \end{aligned} \tag{1}$$

where $E_{11}^{\mathrm{CN}}, E_{22}^{\mathrm{CN}}$ and G_{12}^{CN} are the Young's modulii and the shear modulus of the CNT, respectively and V_{CN} and V_m are the volume fraction of the CNT and the matrix, respectively. The volume fractions are related by: $V_{\mathrm{CN}} + V_m = 1$. The CNT efficiency parameters (η_1, η_2, η_3) are introduced to account for the inconsistency in the load transfer between the CNT and the matrix. The values of the efficiency parameters are obtained by matching the elastic modulus of CNT reinforced polymer matrix observed from the MD simulation results with the numerical results obtained from the rule of mixtures.

Three layer sandwich structure. The three layer sandwich structure is made up of a homogeneous core with core thickness h_H and two facesheets with thickness h_f (see Figure 1). The facesheets are assumed to be reinforced with CNTs. We assume the volume fraction V_{CN} for the top facesheet as

$$V_{\mathrm{CN}} = 2\left(\frac{t_1 - z}{t_1 - t_0}\right) V_{\mathrm{CN}}^* \tag{2}$$

and for the bottom facesheet as follows

$$V_{\mathrm{CN}} = 2\left(\frac{z - t_2}{t_3 - t_2}\right) V_{\mathrm{CN}}^* \tag{3}$$

where,

$$V_{\mathrm{CN}}^* = \frac{w_{\mathrm{CN}}}{w_{\mathrm{CN}} + \left(\frac{\rho_{\mathrm{CN}}}{\rho_m}\right)[1 - w_{\mathrm{CN}}]}$$

where w_{CN} is the mass fraction of the nanotube, ρ_{CN} and ρ_m are the mass densities of carbon nanotube and the matrix, respectively. The thermal expansion coefficient in the longitudinal and transverse directions can be expressed as [18]:

$$\begin{aligned} \alpha_{11} &= \alpha_{11}^{\mathrm{CN}} V_{\mathrm{CN}} + \alpha_m V_m \\ \alpha_{22} &= (1 + \nu_{12}^{\mathrm{CN}}) V_{\mathrm{CN}} \alpha_{22}^{\mathrm{CN}} + (1 + \nu_m) V_m \alpha_m - \nu_{12} \alpha_{11} \end{aligned} \tag{4}$$

where $\alpha_{11}^{\mathrm{CN}}, \alpha_{22}^{\mathrm{CN}}$ and α_m are the thermal expansion coefficients for the CNT and the matrix, respectively and ν_{12}^{CN} and ν_m are the Poisson's ratio.

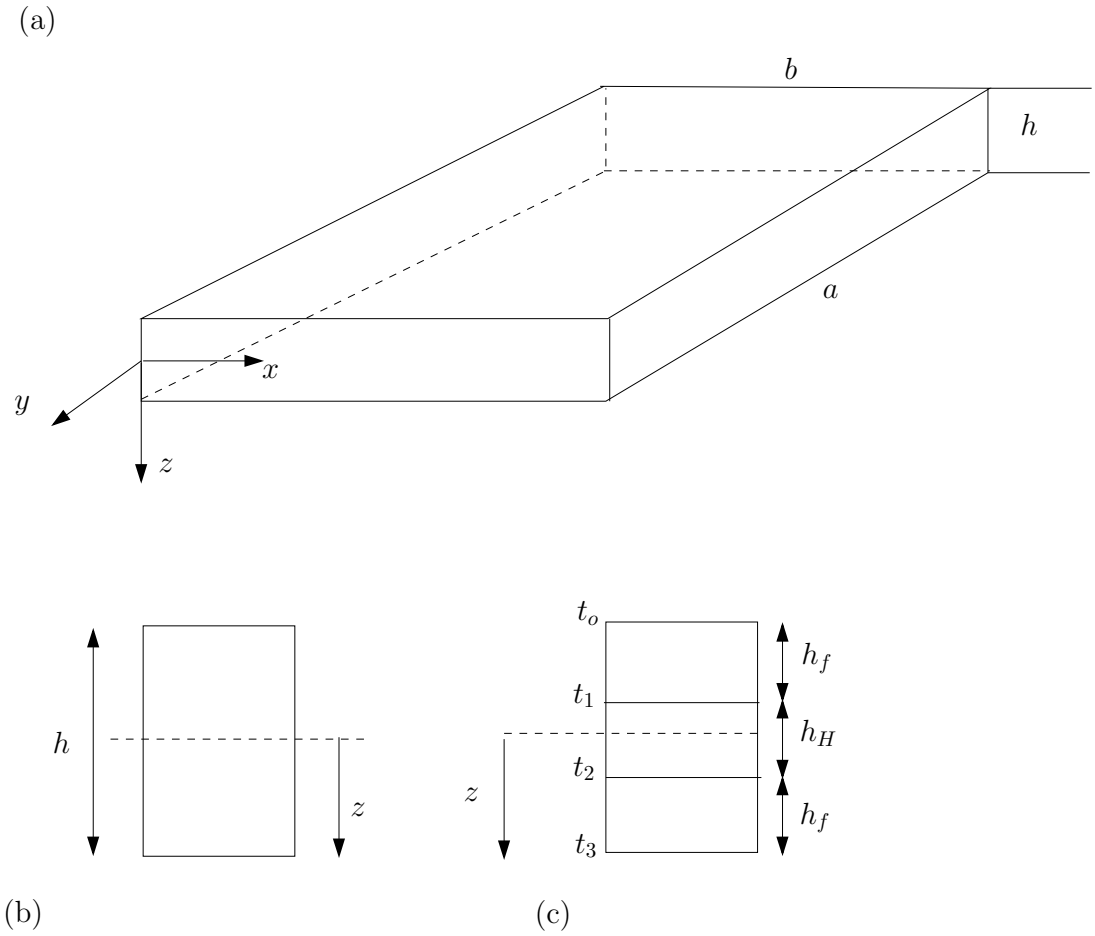

Figure 1: Coordinate system of a rectangular plate: (a) x and y along the in-plane directions and z along the thickness direction: (b) single layer plate cross section and (c) sandwich plate made up of three layers, where h_H is the core thickness and h_f is the facesheet thickness. The CNTs are functionally graded in the facesheets.

3. Higher order accurate theory

The sandwich plate is assumed to be made up of three discrete layers with a homogeneous core. The in-plane displacements u_k and v^k, and the transverse displacement w^k for the k^{th} layer, are assumed as [14, 16]:

$$\begin{aligned} u^k(x,y,z,t) &= u_o(x,y,z,t) + z\theta_x(x,y,t) + z^2\beta_x(x,y,t) + z^3\phi_x(x,y,t) + S^k\psi_x(x,y,t) \\ v^k(x,y,z,t) &= v_o(x,y,z,t) + z\theta_y(x,y,t) + z^2\beta_y(x,y,t) + z^3\phi_y(x,y,t) + S^k\psi_y(x,y,t) \\ w^k(x,y,z,t) &= w_o(x,y,t) + zw_1(x,y,t) + z^2\Gamma(x,y,t) \end{aligned} \tag{5}$$

The terms with even powers of z in the in-plane displacements and odd powers of z occurring in the expansion for w^k correspond to the stretching problem. However, the terms with odd powers of z in the in-plane displacements and the even ones in the expression for w^k represent the flexure problem. u_o, v_o and w_o are the displacements of a generic point on the reference surface; θ_x and θ_y are the rotations of the normal to the reference surface about the y and x axes, respectively; $w_1, \beta_x, \beta_y, \Gamma, \phi_x$ and ϕ_y are the higher-order terms in the Taylor's series expansions, defined at the reference surface. ψ_x and ψ_y are generalized variables associated with the zigzag function, S^k. The zigzag function, S^k, as given in [19, 15, 20], is defined by

$$S^k = 2(-1)^k \frac{z_k}{h_k} \tag{6}$$

where z_k is the local transverse coordinate with the origin at the center of the k^{th} layer and h_k is the corresponding layer thickness. Thus, the zigzag function is piecewise linear with values of -1 and 1 alternatively at different interfaces. The 'zig-zag' function, as defined above, takes care of the inclusion of the slope discontinuities of u and v at the interfaces of the sandwich plate as observed in the exact three-dimensional elasticity solutions of thick sandwich functionally graded materials. The main advantage of using such formulation is that such a function is more economical than a discrete layer approach [21, 22].

The strains in terms of mid-plane deformation, rotations of normal and higher order terms associated with displacements are:

$$\boldsymbol{\varepsilon} = \left\{ \begin{array}{c} \boldsymbol{\varepsilon}_{\mathrm{bm}} \\ \boldsymbol{\varepsilon}_s \end{array} \right\} \tag{7}$$

The vector $\boldsymbol{\varepsilon}_{\mathrm{bm}}$ includes the bending and membrane terms of the strain components and vector $\boldsymbol{\varepsilon}_s$ contains the transverse shear strain terms. These strain vectors are defined as:

$$\begin{aligned} \boldsymbol{\varepsilon}_{\mathrm{bm}} &= \left\{ \begin{array}{c} \varepsilon_{xx} \\ \varepsilon_{yy} \\ \varepsilon_{zz} \\ \gamma_{xy} \end{array} \right\} + \left\{ \begin{array}{c} u_{,x} \\ v_{,y} \\ w_{,z} \\ u_{,y} + v_{,x} \end{array} \right\} \\ &= \boldsymbol{\varepsilon}_0 + z\boldsymbol{\varepsilon}_1 + z^2\boldsymbol{\varepsilon}_2 + z^3\boldsymbol{\varepsilon}_3 + S^k\boldsymbol{\varepsilon}_4 \end{aligned} \tag{8}$$

$$\begin{aligned} \boldsymbol{\varepsilon}_s &= \left\{ \begin{array}{c} \gamma_{xz} \\ \gamma_{yz} \end{array} \right\} = \left\{ \begin{array}{c} u_{,z} + w_{,x} \\ v_{,z} + w_{,y} \end{array} \right\} \\ &= \gamma_o + z\gamma_1 + z^2\gamma_2 + S^k_{,z}\gamma_3 \end{aligned} \tag{9}$$

where

$$\boldsymbol{\varepsilon}_o = \left\{ \begin{array}{c} u_{o,x} \\ v_{o,y} \\ w_1 \\ u_{o,y} + v_{o,x} \end{array} \right\}, \qquad \boldsymbol{\varepsilon}_1 = \left\{ \begin{array}{c} \theta_{x,x} \\ \theta_{y,y} \\ 2\Gamma \\ \theta_{x,y} + \theta_{y,x} \end{array} \right\},$$

$$\boldsymbol{\varepsilon}_2 = \left\{ \begin{array}{c} \beta_{x,x} \\ \beta_{y,y} \\ 0 \\ \beta_{x,y} + \beta_{y,x} \end{array} \right\}, \qquad \boldsymbol{\varepsilon}_3 = \left\{ \begin{array}{c} \phi_{x,x} \\ \phi_{y,y} \\ 0 \\ \phi_{x,y} + \phi_{y,x} \end{array} \right\},$$

$$\boldsymbol{\varepsilon}_4 = \left\{ \begin{array}{c} \psi_{x,x} \\ \psi_{y,y} \\ 0 \\ \psi_{x,y} + \psi_{y,x} \end{array} \right\}. \tag{10}$$

and,

$$\gamma_o = \left\{ \begin{array}{c} \theta_x + w_{o,x} \\ \theta_y + w_{o,y} \end{array} \right\}, \qquad \gamma_1 = \left\{ \begin{array}{c} 2\beta_x + w_{1,x} \\ 2\beta_y + w_{1,y} \end{array} \right\},$$

$$\gamma_2 = \left\{ \begin{array}{c} 3\phi_x + \Gamma_{,x} \\ 3\phi_y + \Gamma_{,y} \end{array} \right\}, \qquad \gamma_3 = \left\{ \begin{array}{c} \psi_x S^k_{,z} \\ \psi_y S^k_{,z} \end{array} \right\}. \tag{11}$$

The subscript comma denotes partial derivatives with respect to the spatial coordinate succeeding it. The constitutive relations for an arbitrary layer k can be expressed as:

$$\begin{aligned} \boldsymbol{\sigma} &= \left\{ \begin{array}{ccccc} \sigma_{xx} & \sigma_{yy} & \sigma_{zz} & \sigma_{xz} & \sigma_{yz} \end{array} \right\}^{\mathrm{T}} \\ &= \mathbf{Q^k} \left\{ \begin{array}{cc} \boldsymbol{\varepsilon}_{\mathrm{bm}} & \boldsymbol{\varepsilon}_s \end{array} \right\}^{\mathrm{T}} \end{aligned} \tag{12}$$

where $\mathbf{Q_k}$ is the stiffness coefficient matrix defined as

$$\begin{gathered} Q^k_{11} = \frac{E_{11}}{1 - \nu_{12}\nu_{21}}; \quad Q^k_{22} = \frac{E_{22}}{1 - \nu_{12}\nu_{21}}; \quad Q^k_{12} = \frac{\nu_{21}E_{11}}{1 - \nu_{12}\nu_{21}}; \\ Q^k_{44} = G_{23}; \;\; Q^k_{55} = G_{13}; \;\; Q^k_{66} = G_{12}; Q^k_{16} = Q^k_{26} = 0. \end{gathered} \tag{13}$$

For the homogeneous core, the shear modulus G is related to the Youngs's modulus by: $E = 2G(1 + \nu)$. The governing equations of motion are obtained by applying Lagrangian equations of motion given by

$$\frac{d}{dt}\left[\frac{\partial(T-U)}{\partial \dot{\delta}_i}\right] - \left[\frac{\partial(T-U)}{\partial \delta_i}\right] = 0, \qquad i = 1, 2, \cdots, n \tag{14}$$

where δ_i is the vector of degrees of freedom and T is the kinetic energy of the plate given by:

$$T(\delta) = \frac{1}{2}\iint \left[\sum_{k=1}^{n} \int_{h_k}^{h_{k+1}} \rho_k \left\{ \begin{array}{ccc} \dot{u}_k & \dot{v}_k & \dot{w}_k \end{array} \right\} \left\{ \begin{array}{ccc} \dot{u}_k & \dot{v}_k & \dot{w}_k \end{array} \right\}^{\mathrm{T}} dz \right] dxdy \tag{15}$$

where ρ_k is the mass density of the k^{th} layer, h_k and h_{k+1} are the z coordinates corresponding to the bottom and

top surfaces of the k^{th} layer. The strain energy function U is given by

$$U(\delta) = \frac{1}{2}\iint \left[\sum_{k=1}^{n}\int_{h_k}^{h_{k+1}} \boldsymbol{\sigma}^{\mathrm{T}}\boldsymbol{\varepsilon}\; dz\right] dxdy - \iint \mathbf{q}w\; dxdy \tag{16}$$

where $\mathbf{q}$ is the distributed force acting on the top surface of the plate. Substituting Equations (16) and (15) in Equation (14), one obtains the following governing equations for static deflection by neglecting the inertia terms and free vibration of plate.

Static deflection.

$$\mathbf{K}\boldsymbol{\delta} = \mathbf{f} \tag{17}$$

Free vibration.

$$\mathbf{M}\ddot{\boldsymbol{\delta}} + \mathbf{K}\boldsymbol{\delta} = \mathbf{0} \tag{18}$$

where $\mathbf{M}$ is the mass matrix, $\mathbf{K}$ is the stiffness matrix and $\mathbf{f}$ is the external force vector. In the present study, while performing the integration, terms having thickness co-ordinate z are integrated with higher order Gaussian quadrature, because the material properties vary continuously through the thickness. The terms containing x and y are evaluated using full integration with 3×3 Gauss integration rule. The frequencies and mode shapes are obtained from Equation (18) using the standard generalized eigenvalue algorithm.

4. Element description

In this paper, $\mathcal{C}^o$ continuous, eight-noded serendipity quadrilateral shear flexible plate element is used. The finite element represented as per the kinematics based on Equation (5) is referred to as HSDT13 with cubic variation. The 13 dofs are: $(u_o, v_o, w_o, \theta_x, \theta_y, w_1, \beta_x, \beta_y, \Gamma, \phi_x, \phi_y, \psi_x, \psi_y)$. Five more alternate discrete models are proposed to study the influence of higher-order terms in the displacement functions, whose displacement fields are deduced from the original element by deleting the appropriate degrees of freedom. These alternate models, and the corresponding degrees of freedom are listed in Table 1

Table 1: Alternate eight-noded finite element models

Finite element model	Degrees of freedom per node
HSDT13	$u_o, v_o, w_o, \theta_x, \theta_y, w_1, \beta_x, \beta_y, \Gamma, \phi_x, \phi_y, \psi_x, \psi_y$
HSDT11A	$u_o, v_o, w_o, \theta_x, \theta_y, \beta_x, \beta_y, \phi_x, \phi_y, \psi_x, \psi_y$
HSDT11B	$u_o, v_o, w_o, \theta_x, \theta_y, w_1, \beta_x, \beta_y, \Gamma, \phi_x, \phi_y$
HSDT9	$u_o, v_o, w_o, \theta_x, \theta_y, \beta_x, \beta_y, \phi_x, \phi_y$
TSDT7	$u_o, v_o, w_o, \theta_x, \theta_y, \beta_x, \beta_y$
FSDT5	$u_o, v_o, w_o, \theta_x, \theta_y$

5. Numerical results and discussion

In this section, we present the static response and the natural frequencies of sandwich plates with homogeneous core and CNT reinforced facesheets using the eight-noded shear flexible quadrilateral element. The effect of plate side-to-thickness ratio, thermal environment, CNT volume fraction on the global response is numerically studied. In this study, only simply supported boundary conditions are considered and are as follows:

$$u_o = w_o = \theta_x = w_1 = \Gamma = \beta_x = \phi_x = \psi_x = 0, \quad \text{on } y = 0, b$$
$$v_o = w_o = \theta_y = w_1 = \Gamma = \beta_y = \phi_y = \psi_y = 0, \quad \text{on } x = 0, a \tag{19}$$

where a and b refer to the length and width of the plate, respectively. The transverse shear stresses are evaluated by integrating the three-dimensional equilibrium equations for all types of elements. For the present study, two different core-to-facesheet thickness h_H/h_f = 2,6 and two thickness ratios a/h (5,10) are considered.

Material properties. For all the numerical studies presented below, unless mentioned otherwise, we employ Poly methyl methacrylate (PMMA) as the matrix in which the CNTs are used as reinforcements. The material properties of which are assumed to be ρ_m = 1150 Kg/m^3, ν_m = 0.34, α_m = 45(1+0.0005ΔT) $\times$ 10^{-6}/K and E_m = (3.52-0.0034T) GPa in which $T = T_o + \Delta T$ and T_o = 300K. Single walled CNTs are used as reinforcements and the material properties at different temperatures are given in Table 2. The following CNT efficiency parameters are used [18]: η_1 = 0.137, η_2 = 1.002 and η_3 = 0.715 for V^*_{CN} = 0.12; η_1 = 0.142, η_2 = 1.626 and η_3 = 1.138 for V^*_{CN} = 0.17 and η_1 = 0.141, η_2 = 1.585 and η_3 = 1.109 for V^*_{CN} = 0.28. For this study, we assume that $G_{13} = G_{12}$ and $G_{23} = 1.2\ G_{12}$. For the homogeneous core, we use Ti-6Al-4V Titanium alloy. The properties are: α_H = 7.5788(1+6.638$\times10^{-4}T$ - 3.147$\times10^{-6}T^2$)$\times10^{-6}$K, Young's modulus, $E_{_H}$ = 122.56(1-4.586$\times10^{-4}T$) GPa, Poisson's ratio $\nu_{_H}$ = 0.29 and mass density $\rho_{_H}$ = 4429 Kg/m^3.

Table 2: Temperature dependent material properties for $(10, 10)$ SWCNT [18].

Temperature	E_{11}^{CN}	E_{22}^{CN}	G_{12}^{CN}	α_{11}^{CN}	α_{22}^{CN}
K	(TPa)	(TPa)	(TPa)	($\times10^{-6}$/K)	($\times10^{-6}$/K)
300	5.6466	7.0800	1.9445	3.4584	5.1682
500	5.5308	6.9348	1.9643	4.5361	5.0189
700	5.4744	6.8641	1.9644	4.6677	4.8943

5.1. Static analysis

The static analysis is conducted for carbon nanotube reinforced functionally graded sandwich plate with homogeneous core. The following two types of mechanical loading are considered:

- Mechanical loading
  - Sinusoidal loading: $q(x, y) = q_o \sin\frac{\pi x}{a} \sin\frac{\pi y}{b}$,
  - Uniformly distributed loading: $q(x, y) = q_o$.
- Thermal loading: $T(x, y) = T_o\left(\frac{2z}{h}\right) \sin\frac{\pi x}{a} \sin\frac{\pi y}{b}$

where q_o and T_o are the amplitude of the mechanical load and the thermal load, respectively. The physical quantities are nondimensionalized by relations, unless stated otherwise:

$$(\overline{u}, \overline{v}) = \frac{100E_{_H}}{q_o h S^3}(u, v)$$
$$\overline{w} = \frac{100E_H}{q_o h S^4} w$$
$$\overline{\sigma}_{xx} = \frac{\sigma_{xx}}{q_o S^2}$$
$$\overline{\sigma}_{xz} = \frac{\sigma_{xz}}{q_o S} \tag{20}$$

for the applied mechanical load and by

$$
\begin{aligned}
(\overline{u},\overline{v}) &= \frac{1}{10h\alpha_H T_o S}(u,v)\\
\overline{w} &= \frac{1}{h\alpha_H T_o h S^4} w\\
\overline{\sigma}_{xx} &= \frac{\sigma_{xx}}{100 E_H \alpha_H T_o}\\
\overline{\sigma}_{xz} &= \frac{\sigma_{xz}}{10 E_H \alpha_H T_o}
\end{aligned}
\tag{21}
$$

for the applied thermal load, where the $E_{_H}, \alpha_{_H}$ are the Young's modulus and the co-efficient of thermal expansion corresponding to the homogeneous core, evaluated at $T_o = 300$K and $S = a/h$.

Before proceeding to the detailed analysis of the static response of the sandwich plate for the applied mechanical load, the present formulation is validated against available solutions in the literature. In this case, only one layer is considered. The CNTs are either uniformly distributed or functionally graded along the thickness direction, given by:

$$
V_{\mathrm{CN}}(z) = \begin{cases} V^*_{\mathrm{CN}} & \text{UD} \\ \left(1+\frac{2z}{h}\right) V^*_{\mathrm{CN}} & \text{FG-V Type} \\ 2\left(\frac{2|z|}{h}\right) V^*_{\mathrm{CN}} & \text{FG-X Type} \end{cases}
\tag{22}
$$

The effective material properties, viz., Young's modulus, Poisson's ratio and the mass density are estimated from Equation (1). The effect of type of CNT volume fraction distribution is also considered. PmPV [8] is considered as the matrix with material properties: $E_m = 2.1$ GPa at room temperature (300K), $\nu_m = 0.34$. The SWCNTs are chosen as the reinforcements and the material properties for the SWCNT are taken from [8] and given in Table 2. The CNT efficiency parameters η_j are determined according to the effective properties of CNTRCs available by matrching the Young's moduli E_1 and E_2 with the counterparts computed by rule of mixtures. In this study, the efficiency parameters are: $\eta_1 = 0.149$ and $\eta_2 = 0.934$ for the case of $V^*_{\mathrm{CN}} = 0.11$; $\eta_1 = 0.150$ and $\eta_2 = 0.941$ for the case of $V^*_{\mathrm{CN}} = 0.14$ and $\eta_1 = 0.149$ and $\eta_2 = 1.381$ for the case of $V^*_{\mathrm{CN}} = 0.17$. It is assumed that $\eta_2 = \eta_3$ for this study.

Table 3: Convergence of maximum center deflection $w_c = -w_o/h\times 10^{-2}$ with mesh size for a simply supported square plate subjected to uniformly distributed load with $a/h = 20$. The volume fraction of the CNT is $V^*_{\mathrm{CN}} = 0.14$.

Mesh	FSDT5			HSDT11B		
	UD	FG-V	FG-X	UD	FG-V	FG-X
4×4	3.0174	4.0418	2.2710	3.0172	4.0959	2.2764
6×6	3.0018	4.0209	2.2593	3.0017	4.0748	2.2647
8×8	2.9993	4.0176	2.2574	2.9873	4.0552	2.2538
16×16	2.9993	4.0176	2.2574	2.9873	4.0552	2.2538
Ref. [8]	3.0010	4.0250	2.2560	-	-	-

Tables 3 - 4 present the convergence of the maximum center deflection with decreasing mesh size for a simply supported square plate subjected to uniformly distributed load with $a/h = 20$ employing the first- (FSDT5) & higher order (HSDT11B) and with $a/h = 5$ employing the higher-order (HSDT13) structural models. The results of the first-order shear deformation theory (FSDT5) employed here is compared with the available results from the literature [8]. It can be seen that the results from the present formulation are in excellent agreement with the results in the literature and that a 8×8 mesh is found to be adequate to model the full plate, viz., sandwich plate or single layer for the present analysis. The influence of the CNT volume fraction distribution is also studied. It

Table 4: Convergence of maximum center deflection $w_c = -w_o/h \times 10^{-2}$ with mesh size for a simply supported square sandwich plate subjected to sinusoidally distributed mechanical load with $a/h = 5$.

Mesh	$h_H/h_f = 2$	
	$V^*_{\mathrm{CN}} = 0.17$	$V^*_{\mathrm{CN}} = 0.28$
4×4	0.1042	0.0911
6×6	0.1037	0.0907
8×8	0.1036	0.0906
16×16	0.1036	0.0906

is seen that the plate with CNT reinforced in FG-V has the maximum center deflection and the plate with FG-X type of reinforcement has the minimum center deflection.

Next the numerical study is carried out to study the influence of the plate thickness a/h, the core-to-facesheet thickness h_H/h_f and the CNT volume fraction V^*_{CN} on the deflection and the stresses for a plate with sinusoidal loading. Numerical results are tabulated in Tables 5 and 6 for an applied sinusoidal mechanical load and in Tables 7 and 8 for an applied thermal load. It is inferred from these Tables that with increasing the CNT volume fraction V^*_{CN}, the non-dimensionalized displacement decreases whereas the change in the non-dimensionalized stresses however depends on the thickness ratio. Furthermore, the non-dimensionalized displacements and the non-dimensionalized stresses decrease in general with increasing core thickness. This can be attributed to the change in the flexural stiffness due to increase in the core thickness and the addition of CNTs to the facesheets. It can be also noted that the non-dimensionalized displacements and the non-dimensionalized stresses predicted at the neutral surface using HSDT13, HSDT11A and HSDT11B are different from those of HSDT9, TSDT7 and FSDT5. However, the latter models cannot predict the through thickness stretching effects in the displacements and the stresses.

Through thickness variation of displacements and stresses for $h_H/h_f = 2$ with $a/h = 5$ and $a/b = 1$ is demonstrated considering two locations in the sandwich plate in Figures 2 and 3 for different structural models employed in the present investigation for mechanical and thermal load cases, respectively. A significant difference in the through thickness non-dimensionalized displacements and non-dimensionalized stresses can be seen while adopting different plate theories as noticed in Figures 2 and 3. The main difference among the higher-order theories is in accounting for the slope discontinuity in the in-plane displacements through the thickness whereas it is the inclusion of variation up to cubic term in the in-plane displacements among the lower-order theories. The influence of including the zig-zag function is clearly seen (HSDT13, HSDT11A) as there is a significant change in the material properties through the thickness. However, the shear stress variation predicted adopting HSDT11A and HSDT11B matches with some regions in the thickness direction in comparison with those of HSDT13. It can be concluded that the performance of the structural model with the inclusion of zig-zag function is overall comparable with those of the higher-order model HSDT13 for the mechanical response of the sandwich structures. Similar experimentation of these types of theories for an applied thermal load is presented in Figure 3. The behaviour of HSDT11A and HSDT11B for thermal response is somewhat similar to those of mechanical case. However, it may be opined that the prediction of shear stresses by the structural model with the presence of linear/quadratic terms in the transverse response is overall very close to those of the higher-order model HSDT13 for the thermal response of the sandwich structures.

5.2. Free flexural vibrations

Next, the free vibration characteristics of sandwich plate is numerically studied. In all cases, we present the non-dimensionalized free flexural frequency defined as:

$$\Omega = \frac{\omega a^2}{h}\sqrt{\frac{\rho_{_H}}{E_{_H}}} \tag{23}$$

Table 5: Deflections and stresses for a simply supported square sandwich plates with homogeneous core and CNT reinforced face-sheets subjected to sinusoidally distributed load (mechanical load) with $a/h = 5$ and 10. The volume fraction of the CNT, $V^*_{\mathrm{CN}} = 0.17$ is assumed to functionally graded. The displacements and stresses are reported for the following locations: $\overline{u} = \overline{u}(0, b/2, h/2)$, $\overline{w} = \overline{w}(a/2, b/2, h/2)$, $\overline{\sigma}_{xx} = \overline{\sigma}_{xx}(a/2, a/2, h/2)$ and $\overline{\sigma}_{xz} = \overline{\sigma}_{xz}(0, b/2, 0)$.

a/h	Element	$h_H/h_f = 2$				$h_H/h_f = 6$			
		$\overline{u}$	$\overline{w}$	$\overline{\sigma}_{xx}$	$\overline{\sigma}_{xz}$	$\overline{u}$	$\overline{w}$	$\overline{\sigma}_{xx}$	$\overline{\sigma}_{xz}$
5	HSDT13	0.5463	0.1036	0.4476	0.4021	0.5275	0.0533	0.4247	0.3154
	HSDT11A	0.5617	0.1084	0.4715	0.3985	0.5390	0.0557	0.4491	0.3147
	HSDT11B	0.6701	0.0813	0.5496	0.3960	0.6725	0.0504	0.5448	0.3168
	HSDT9	0.6883	0.0847	0.5747	0.3926	0.6887	0.0526	0.5727	0.3162
	TSDT7	0.9108	0.0744	0.7578	0.3798	0.6840	0.0523	0.5687	0.3155
	FSDT5	0.9042	0.0773	0.7525	0.3791	0.6800	0.0538	0.5654	0.3149
10	HSDT13	0.8132	0.0738	0.6717	0.3906	0.6535	0.0470	0.5383	0.3183
	HSDT11A	0.8189	0.0749	0.6819	0.3891	0.6574	0.0477	0.5466	0.3179
	HSDT11B	0.8663	0.0658	0.7155	0.3884	0.6968	0.0461	0.5738	0.3188
	HSDT9	0.8721	0.0668	0.7255	0.3870	0.7010	0.0468	0.5827	0.3184
	TSDT7	0.9359	0.0637	0.7779	0.3828	0.6994	0.0467	0.5813	0.3181
	FSDT5	0.9341	0.0645	0.7765	0.3826	0.6983	0.0471	0.5804	0.3179

Table 6: Deflections and stresses for a simply supported square sandwich plates with homogeneous core and CNT reinforced face-sheets subjected to sinusoidally distributed load (mechanical load) with $a/h = 5$ and 10. The volume fraction of the CNT, $V^*_{\mathrm{CN}} = 0.28$ is assumed to functionally graded. The displacements and stresses are reported for the following locations: $\overline{u} = \overline{u}(0, b/2, h/2)$, $\overline{w} = \overline{w}(a/2, b/2, h/2)$, $\overline{\sigma}_{xx} = \overline{\sigma}_{xx}(a/2, a/2, h/2)$ and $\overline{\sigma}_{xz} = \overline{\sigma}_{xz}(0, b/2, 0)$.

a/h	Element	$h_H/h_f = 2$				$h_H/h_f = 6$			
		$\overline{u}$	$\overline{w}$	$\overline{\sigma}_{xx}$	$\overline{\sigma}_{xz}$	$\overline{u}$	$\overline{w}$	$\overline{\sigma}_{xx}$	$\overline{\sigma}_{xz}$
5	HSDT13	0.3603	0.0906	0.4809	0.3970	0.4118	0.0481	0.5378	0.3167
	HSDT11A	0.3705	0.0945	0.5058	0.3933	0.4201	0.0502	0.5691	0.3160
	HSDT11B	0.4343	0.0659	0.5800	0.3903	0.5486	0.0441	0.7220	0.3186
	HSDT9	0.4456	0.0683	0.6051	0.3870	0.5610	0.0458	0.7585	0.3180
	TSDT7	0.6314	0.0573	0.8542	0.3724	0.5671	0.0455	0.7666	0.3167
	FSDT5	0.6260	0.0604	0.8472	0.3715	0.5626	0.0471	0.7606	0.3158
10	HSDT13	0.5584	0.0574	0.7496	0.3846	0.5375	0.0404	0.7190	0.3205
	HSDT11A	0.5624	0.0583	0.7614	0.3830	0.5406	0.0410	0.7307	0.3201
	HSDT11B	0.5940	0.0485	0.7973	0.3821	0.5801	0.0391	0.7764	0.3212
	HSDT9	0.5979	0.0492	0.8086	0.3807	0.5835	0.0397	0.7885	0.3208
	TSDT7	0.6519	0.0458	0.8810	0.3760	0.5848	0.0396	0.7902	0.3202
	FSDT5	0.6504	0.0466	0.8791	0.3757	0.5835	0.0400	0.7885	0.3199

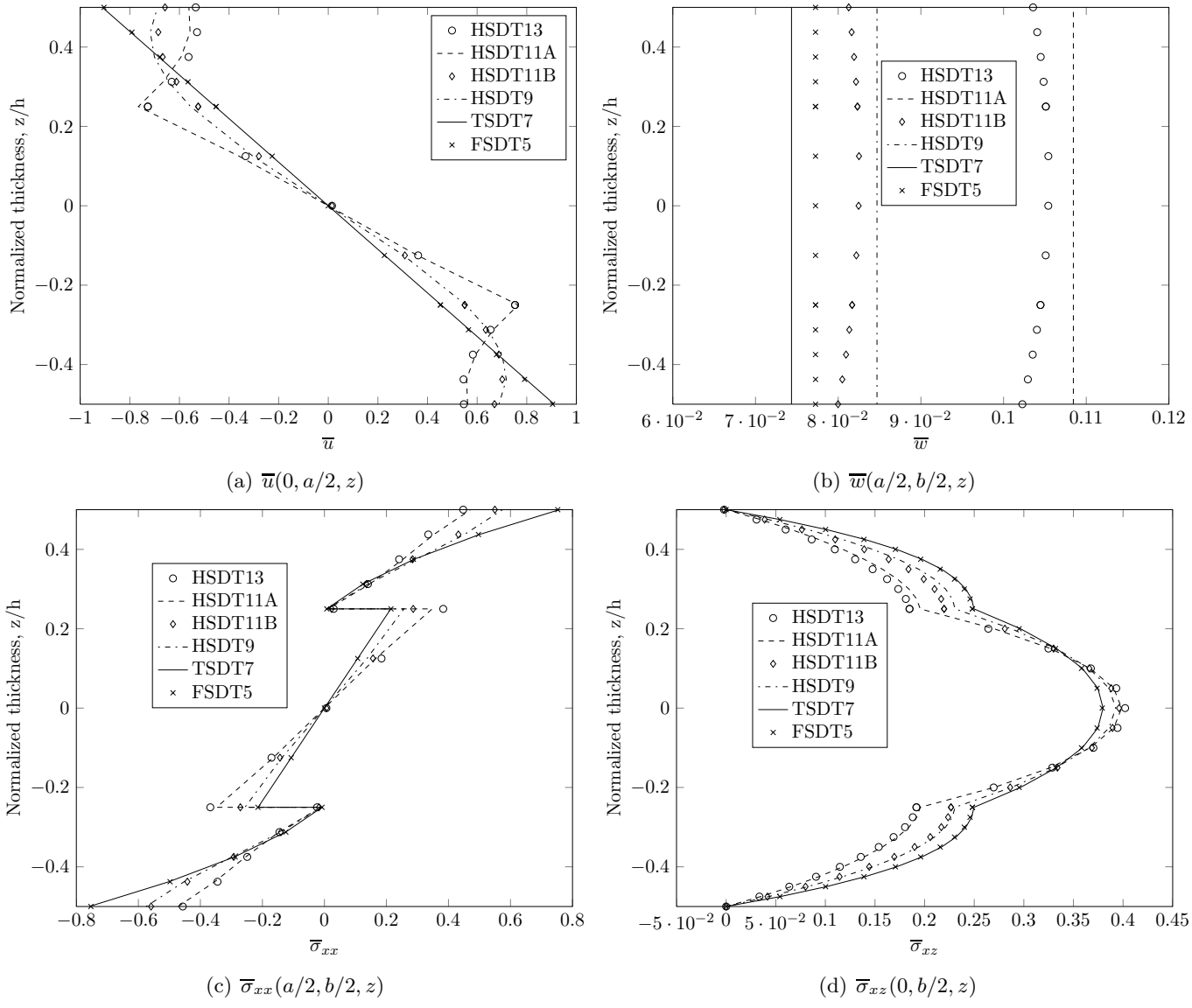

(a) $\overline{u}(0, a/2, z)$

(b) $\overline{w}(a/2, b/2, z)$

(c) $\overline{\sigma}_{xx}(a/2, b/2, z)$

(d) $\overline{\sigma}_{xz}(0, b/2, z)$

Figure 2: Displacements and stresses through the thickness for the square plates with simply supported edges with $a/h = 5$, $h_H/h_f = 2$ and $V^*_{\mathrm{CN}} = 0.17$ and the CNT distribution is FG-X. The plate is subjected to a mechanical load $q(x, y) = q_o \sin(\pi x/a) \sin(\pi y/b)$

Table 7: Deflections and stresses for a simply supported square sandwich plates with homogeneous core and CNT reinforced face-sheets subjected to sinusoidally distributed load (thermal load) with $a/h = 5$ and 10. The volume fraction of the CNT, $V^*_{\mathrm{CN}} = 0.17$ is assumed to functionally graded. The displacements and stresses are reported for the following locations: $\overline{u} = \overline{u}(0, b/2, h/2)$, $\overline{w} = \overline{w}(a/2, b/2, h/2)$, $\overline{\sigma}_{xx} = \overline{\sigma}_{xx}(a/2, a/2, h/2)$ and $\overline{\sigma}_{xz} = \overline{\sigma}_{xz}(0, b/2, -h/6)$.

a/h	Element	$h_H/h_f = 2$				$h_H/h_f = 6$			
		$\overline{u}$	$\overline{w}$	$\overline{\sigma}_{xx}$	$\overline{\sigma}_{xz}$	$\overline{u}$	$\overline{w}$	$\overline{\sigma}_{xx}$	$\overline{\sigma}_{xz}$
5	HSDT13	0.1357	0.6106	0.1133	0.0893	0.0907	0.3786	0.0757	0.0620
	HSDT11A	0.1350	0.6149	0.1121	0.0846	0.0901	0.3755	0.0748	0.0532
	HSDT11B	0.1308	0.6953	0.1093	0.0886	0.0730	0.4137	0.0610	0.0612
	HSDT9	0.1305	0.6965	0.1084	0.0839	0.0730	0.4108	0.0607	0.0525
	TSDT7	0.1206	0.7417	0.1003	0.0836	0.0682	0.4089	0.0567	0.0525
	FSDT5	0.1209	0.7383	0.1005	0.0837	0.0688	0.4075	0.0571	0.0527
10	HSDT13	0.1242	0.7070	0.1038	0.0308	0.0725	0.4035	0.0606	0.0159
	HSDT11A	0.1243	0.7122	0.1033	0.0306	0.0725	0.4042	0.0603	0.0147
	HSDT11B	0.1222	0.7376	0.1021	0.0303	0.0672	0.4143	0.0562	0.0155
	HSDT9	0.1224	0.7409	0.1018	0.0301	0.0673	0.4149	0.0560	0.0143
	TSDT7	0.1196	0.7545	0.0994	0.0298	0.0661	0.4144	0.0550	0.0141
	FSDT5	0.1197	0.7536	0.0995	0.0298	0.0663	0.4140	0.0551	0.0142

Table 8: Deflections and stresses for a simply supported square sandwich plates with homogeneous core and CNT reinforced face-sheets subjected to sinusoidally distributed load (thermal load) with $a/h = 5$ and 10. The volume fraction of the CNT, $V^*_{\mathrm{CN}} = 0.28$ is assumed to functionally graded. The displacements and stresses are reported for the following locations: $\overline{u} = \overline{u}(0, b/2, h/2)$, $\overline{w} = \overline{w}(a/2, b/2, h/2)$, $\overline{\sigma}_{xx} = \overline{\sigma}_{xx}(a/2, a/2, h/2)$ and $\overline{\sigma}_{xz} = \overline{\sigma}_{xz}(0, b/2, -h/6)$.

a/h	Element	$h_H/hf = 2$				$h_H/hf = 6$			
		$\overline{u}$	$\overline{w}$	$\overline{\sigma}_{xx}$	$\overline{\sigma}_{xz}$	$\overline{u}$	$\overline{w}$	$\overline{\sigma}_{xx}$	$\overline{\sigma}_{xz}$
5	HSDT13	0.1145	0.5642	0.1552	0.1155	0.0870	0.3884	0.1179	0.0768
	HSDT11A	0.1142	0.5672	0.1542	0.1111	0.0868	0.3863	0.1172	0.0683
	HSDT11B	0.1123	0.6351	0.1523	0.1149	0.0748	0.4246	0.1014	0.0761
	HSDT9	0.1121	0.6348	0.1515	0.1105	0.0749	0.4228	0.1012	0.0675
	TSDT7	0.1076	0.6615	0.1454	0.1104	0.0709	0.4237	0.0958	0.0675
	FSDT5	0.1077	0.6581	0.1456	0.1105	0.0713	0.4217	0.0964	0.0677
10	HSDT13	0.1090	0.6379	0.1478	0.0438	0.0736	0.4186	0.0998	0.0229
	HSDT11A	0.1092	0.6425	0.1476	0.0436	0.0738	0.4199	0.0997	0.0217
	HSDT11B	0.1079	0.6633	0.1464	0.0433	0.0698	0.4304	0.0946	0.0224
	HSDT9	0.1082	0.6662	0.1463	0.0432	0.0700	0.4315	0.0946	0.0212
	TSDT7	0.1069	0.6744	0.1445	0.0430	0.0690	0.4318	0.0932	0.0211
	FSDT5	0.1069	0.6735	0.1446	0.0430	0.0691	0.4312	0.0934	0.0211

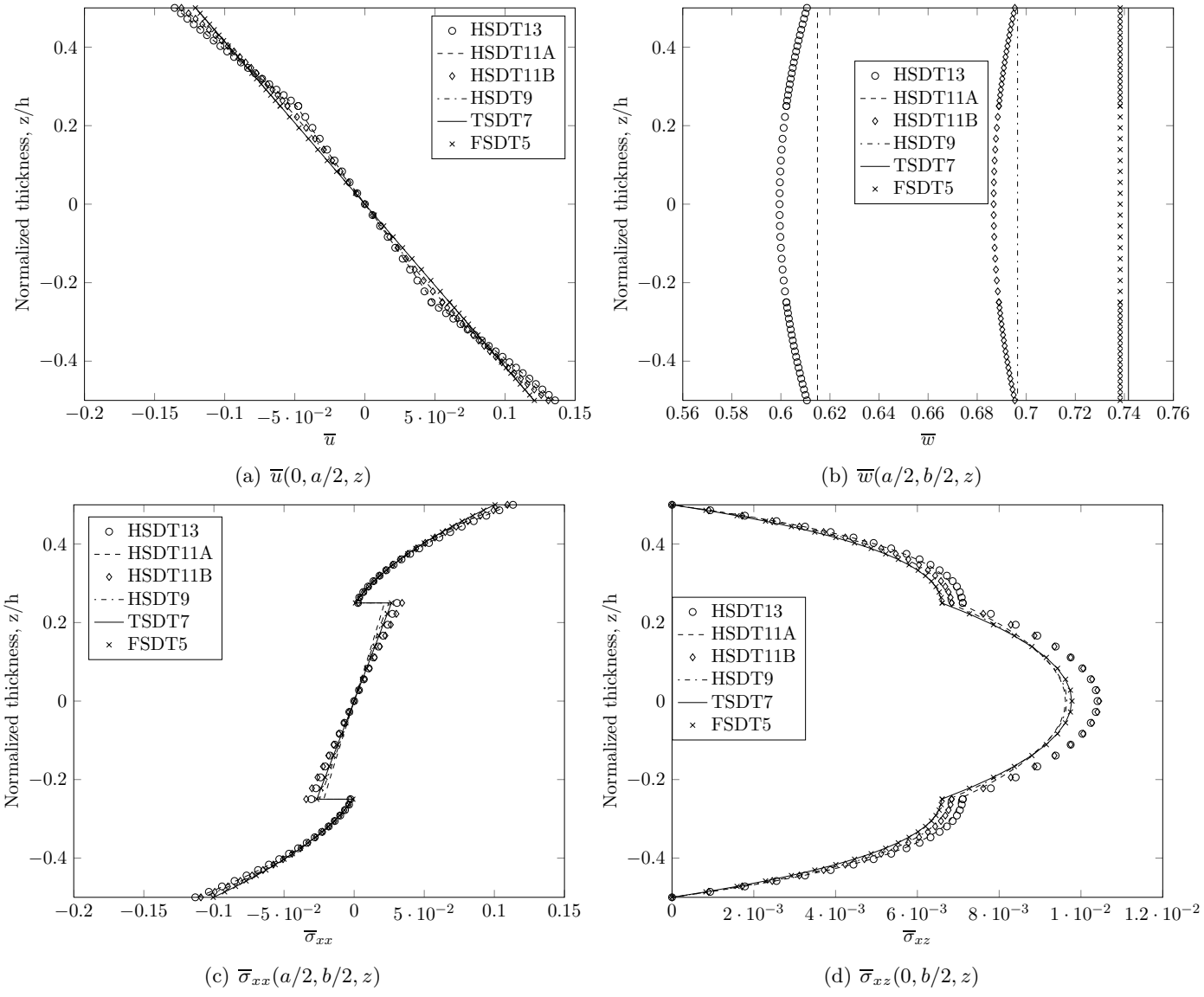

(a) $\overline{u}(0, a/2, z)$

(b) $\overline{w}(a/2, b/2, z)$

(c) $\overline{\sigma}_{xx}(a/2, b/2, z)$

(d) $\overline{\sigma}_{xz}(0, b/2, z)$

Figure 3: Displacements and stresses through the thickness for the square plates with simply supported edges with $a/h = 5$, $h_H/h_f = 2$ and $V^*_{\mathrm{CN}} = 0.28$ and the CNT distribution is FG-X. The plate is subjected to a thermal load $T(x, y) = T_o\left(\frac{2z}{h}\right)\sin(\pi x/a)\sin(\pi y/b)$

where ω is the natural frequency, ρ_H, E_H are the mass density and the Young's modulus of the homogeneous core evaluated at $T_o = 300$K. Before proceeding with a detailed numerical study on the effect of CNT volume fraction, temperature effects, the core thickness and the plate thickness on the fundamental frequency, the formulation developed herein is validated against available results in the literature [18], which is based on the first order shear deformation theory. Table 9 presents the non-dimensionalized frequency of sandwich plates with CNT reinforced facesheets in thermal environment based on various plate theories. For this study, a 8×8 structures Q8 mesh was found to be adequate to model the entire plate. It is seen that the results from the present formulation are in very good agreement with the results available in the literature [18]. The effect of volume fraction of the CNTs, V^*_{CN} and core-to-facesheet thickness ratio is also shown. With increasing temperature, the non-dimensionalized frequency decreases, whilst it increases with increasing volume fraction and core-to-facesheet thickness as expected.

Table 9: Comparison of fundamental frequency $\Omega = \omega \frac{a^2}{h}\sqrt{\frac{\rho_H}{E_H}}$ for sandwich plates with CNT reinforced facesheets in thermal environment with $a/b = 1$ and $a/h = 20$ for various core-to-facesheet thickness (h_H/h_f =4,6) and CNT volume fraction V^*_{CNT}. The CNTs are assumed to the functionally graded, i.e., FGX.

Temperature	Theory	$h_H/h_f = 4$			$h_H/h_f = 6$		
		$V^*_{\mathrm{CN}} = 0.12$	$V^*_{\mathrm{CN}} = 0.17$	$V^*_{\mathrm{CN}} = 0.28$	$V^*_{\mathrm{CN}} = 0.12$	$V^*_{\mathrm{CN}} = 0.17$	$V^*_{\mathrm{CN}} = 0.28$
300	HSDT13	4.6518	5.0381	5.6422	4.8992	5.1753	5.6278
	HSDT11A	4.6508	5.0366	5.6394	4.8980	5.1737	5.6253
	HSDT11B	4.6803	5.0683	5.6980	4.9111	5.1886	5.6534
	HSDT9	4.6793	5.0669	5.6955	4.9099	5.1871	5.6510
	TSDT7	4.6808	5.0697	5.7025	4.9111	5.1881	5.6524
	FSDT5	4.6765	5.0639	5.6935	4.9066	5.1826	5.6448
	Ref. [18]	4.6845	5.0763	5.7131	4.9119	5.1905	5.6569
500	HSDT13	4.4425	4.8244	5.4238	4.6662	4.9408	5.3956
	HSDT11A	4.4416	4.8232	5.4216	4.6651	4.9395	5.3936
	HSDT11B	4.4809	4.8658	5.5005	4.6823	4.9590	5.4308
	HSDT9	4.4801	4.8647	5.4985	4.6813	4.9577	5.4289
	TSDT7	4.4819	4.8681	5.5075	4.6824	4.9587	5.4305
	FSDT5	4.4776	4.8623	5.4982	4.6779	4.9533	5.4227
	Ref. [18]	4.4853	4.8743	5.5180	4.6831	4.9609	5.4350

Next, the influence of the plate side-to-thickness ratio, a/h, the volume fraction of the CNTs V^*_{CN}, the CNT distribution, the core-to-facesheet thickness ratio h_H/h_f and the temperature on the fundamental frequency is numerically studied by employing various plate theories. The results are tabulated in Table 10. It can be opined from Table 10 that the performance of higher-order theories, HSDT13 and HSDT11A are comparable as demonstrated in static bending case. The CNTs are reinforced functionally graded through the thickness according to Equations (2) - (3). It can be seen that the non-dimensionalized frequency (Ω) of the plate increases with decrease in the plate thickness, whilst increases with increasing CNT volume fraction and the core-to-facesheet thickness. This can be attributed to the local flexibility due to decreasing plate thickness and increasing the homogeneous core thickness. The influence of the temperature and the type of CNT distribution, viz, UD/FGX on the non-dimensionalized frequency for a square plate with $a/h = 5$ is shown in Table 11. For all the plate theories considered in this study, it is seen that the non-dimenisonalized frequency increases with the increase in the homogeneous core thickness and decreases with increasing temperature. It can be observed from Table 11 that for $a/h = 10$, the non-dimesninoalized frequency increases when the CNT distribution is changed from UD to FGX, irrespective of the structural model employed. However, for $a/h = 5$, structural models HSDT11B, HSDT9, TSDT7, FSDT5 predicts increasing fundamental frequency when changing the CNT distribution from UD to FGX, whilst HSDT13 and HSDT11A predicts decrease in the frequency.

Table 10: Influence of the plate thickness a/h, the volume fraction of the nanotubes $V^a_{\rm CN}st$ and core-to-the thickness ratio h_H/h_f on the fundamental frequency parameter Ω for a simply supported square sandwich plate with a homogeneous core. The temperature is assumed to be $T_o = 300$K. The CNTs are assumed to the functionally graded, i.e., FGX.

a/h	Element		$h_H/h_f = 2$			$h_H/h_f = 6$	
	Type	$V^*_{\rm CN} = 0.12$	$V^*_{\rm CN} = 0.17$	$V^*_{\rm CN} = 0.28$	$V^*_{\rm CN} = 0.12$	$V^*_{\rm CN} = 0.17$	$V^*_{\rm CN} = 0.28$
5	HSDT13	3.3961	3.7815	4.0457	4.4193	4.6221	4.8681
	HSDT11A	3.3858	3.7714	4.0327	4.4058	4.6097	4.8560
	HSDT11B	3.8434	4.2602	4.7377	4.5334	4.7512	5.0871
	HSDT9	3.8381	4.2554	4.7318	4.5212	4.7402	5.0774
	TSDT7	4.0745	4.5394	5.1622	4.5365	4.7534	5.0935
	FSDT5	4.0164	4.4561	5.0308	4.4820	4.6891	5.0097
10	HSDT13	4.0191	4.5719	5.1744	4.7838	5.0419	5.4336
	HSDT11A	4.0166	4.5688	5.1689	4.7798	5.0378	5.4289
	HSDT11B	4.2753	4.8382	5.6273	4.8264	5.0895	5.5223
	HSDT9	4.2739	4.8364	5.6240	4.8225	5.0857	5.5182
	TSDT7	4.3659	4.9522	5.8245	4.8271	5.0897	5.5232
	FSDT5	4.3472	4.9238	5.7744	4.8100	5.0691	5.4952

Table 11: Influence of the temperature T, plate thickness a/h and the type of CNT distribution, viz., UD/FGX on the fundamental frequency parameter Ω for a simply supported square plate with a homogeneous core with $h_H/h_f = 2$ and $V^*_{\rm CN} = 0.17$.

a/h	Element	UD		FGX	
	Type	$T = 300$K	$T = 500$K	$T =300$K	$T = 500$K
5	HSDT13	3.8203	3.5588	3.7815	3.4910
	HSDT11A	3.8108	3.5492	3.7714	3.4809
	HSDT11B	4.1736	3.9680	4.2602	4.0277
	HSDT9	4.1677	3.9623	4.2554	4.0232
	TSDT7	4.3199	4.1501	4.5394	4.3657
	FSDT5	4.2504	4.0789	4.4561	4.2801
10	HSDT13	4.4397	4.2129	4.5719	4.3092
	HSDT11A	4.4373	4.2105	4.5688	4.3063
	HSDT11B	4.6095	4.4305	4.8382	4.6441
	HSDT9	4.6078	4.4291	4.8364	4.6427
	TSDT7	4.6655	4.5034	4.9522	4.7899
	FSDT5	4.6426	4.4795	4.9238	4.7602

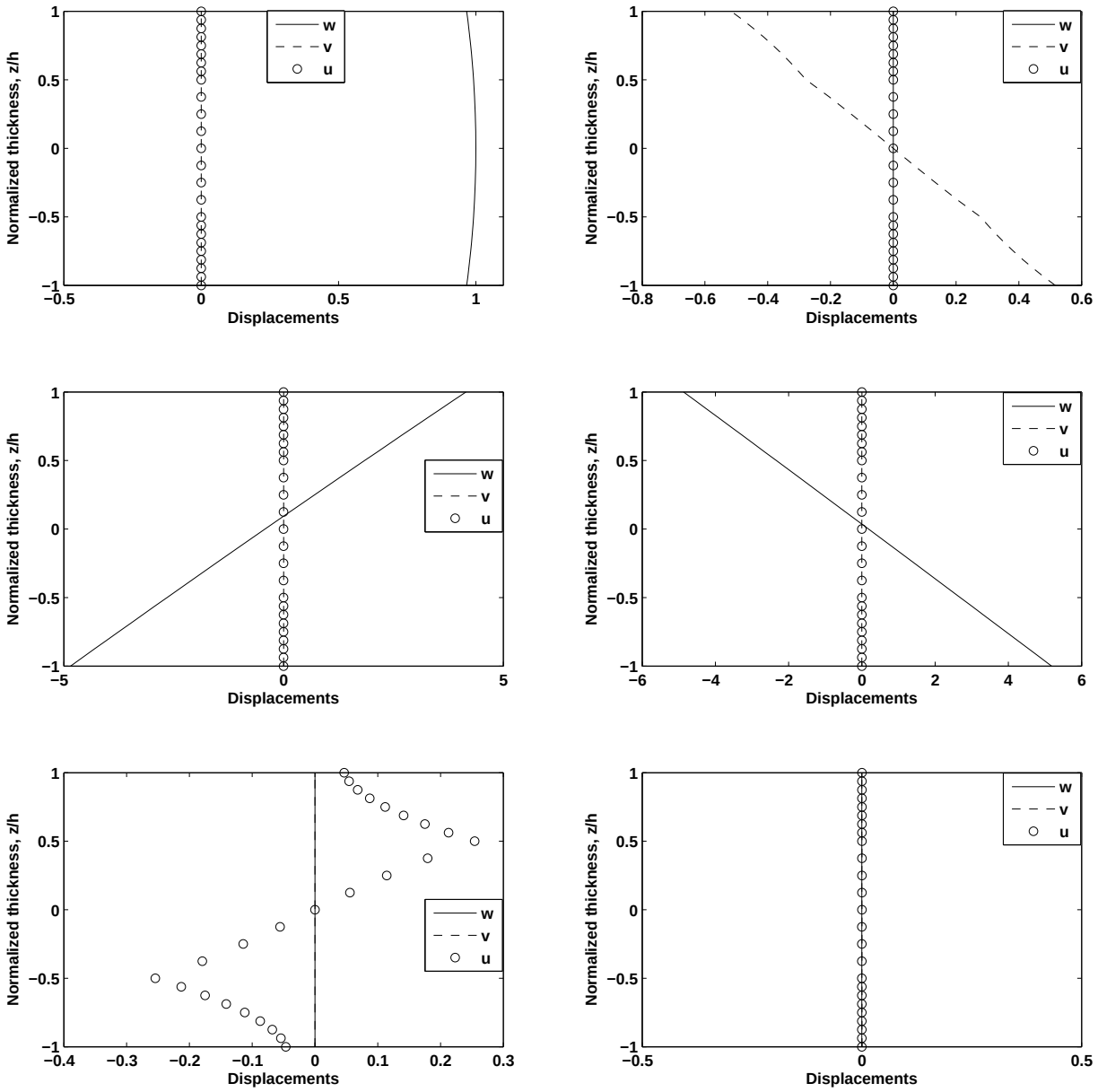

Figure 4: Deflected shapes $u_i(a/2, a/2, z),\ i = x, y, z$ of the six modes for the square plates with simply supported edges with thickness, $a/h = 5$.

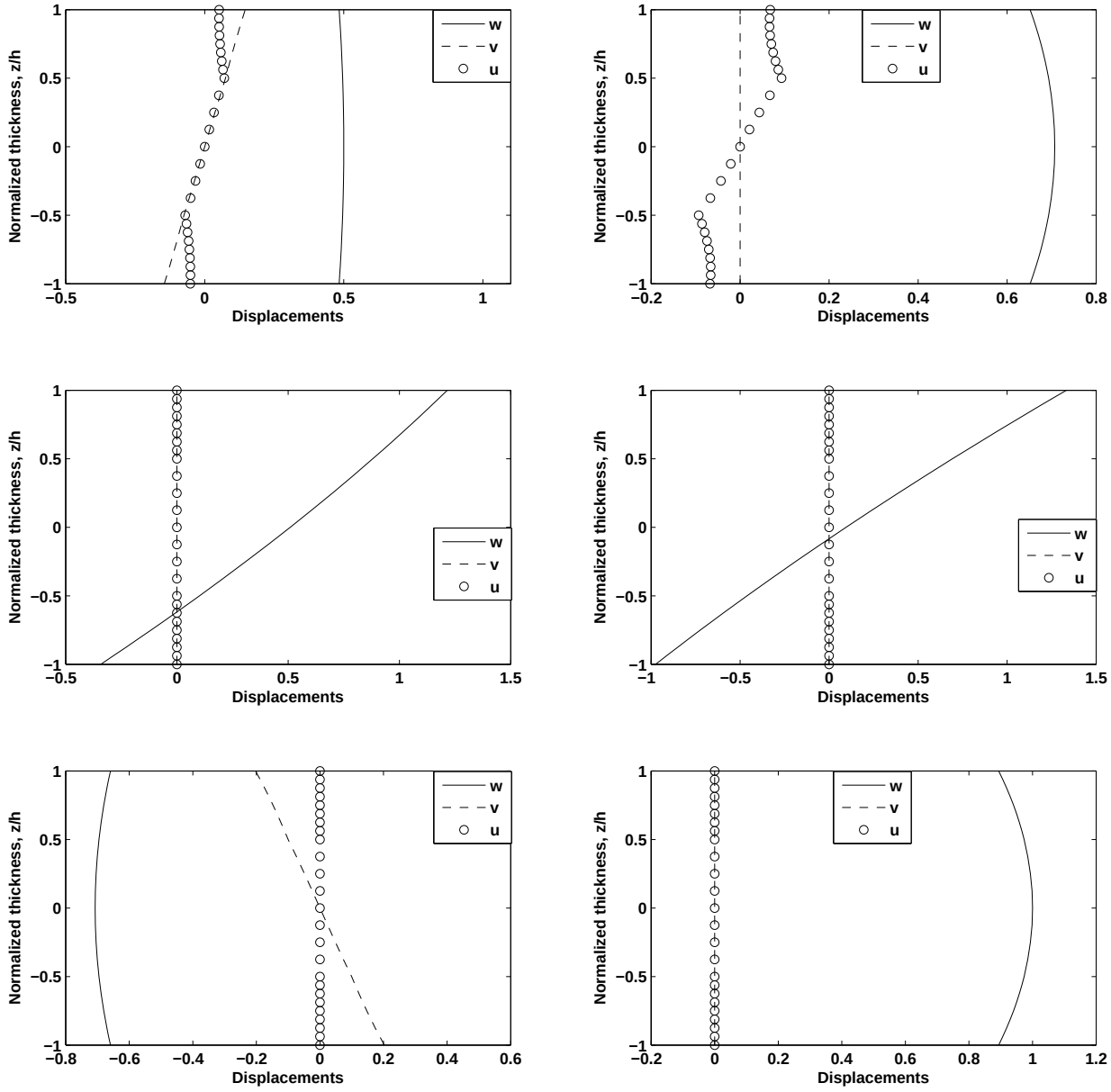

Figure 5: Deflected shapes $u_i(3a/4, 3a/4, z),\ i = x, y, z$ of the six modes for the square plates with simply supported edges with thickness, $a/h = 5$.

Figures 4 - 5 show the relative displacements through the thickness of the sandwich plate for the first six modes using HSDT13. The plate is square simply supported with $h_H/h_f = 2$ and $a/h = 5$. The displacements (u, v, w) are plotted along the lines $(a/2, b/2, z)$ and $(3a/4, 3b/4, z)$, where $h/2 \leq z \leq h/2$. It can be seen from the flexural modes in Figures 4 - 5 where the transverse displacement w is not uniform at the chosen locations exhibit the existence of normal stresses in the thickness direction. In flexural modes 2 – 5 shown in Figure 4, the deflected shape retains the thickness at $(a/2, b/2, z)$ whereas the thickness of the plate is compressed at the other location, i.e., at $(3a/4, 3b/4, z)$ as seen by the modes 1, 2 & 5 in Figure 5. It can be also viewed that the variation of in-plane displacement, in general, is linear or nonlinear, irrespective of the types of modes. Furthermore, there may be a possibility of occurring of extensional mode at some locations. In general, it may be opined that the types of modes in the thickness direction depend on the location in the given sandwich structures.

6. Conclusions

The static and dynamic responses of sandwich plates with CNT reinforced facesheets are studied considering various parameters such as the sandwich type, temperature effects, the thickness ratio and the volume fraction of the CNT. Different plate models are employed in predicting the global structural behaviour and their through thickness variations in the sandwich plate. From a detailed parametric investigation on the effectiveness of higher-order models (HSDT13, HSDT11A and HSDT11B) over the other theories, neglecting the stretching terms in transverse displacement function, the following observations can be made:

- HSDT11A and HSDT11B, to some extent predict the global response of stuctures, irrespective of the type of load, viz., mechanical or thermal. However, there is a variation in evaluating the shear stress through the thickness of the sandwich plates.
- HSDT13 is capable of evaluating the displacements and stresses accurately for the global as well as the local response characteristics of the structure.
- The performance of the higher-order model, HSDT13 for the thick plate is significantly different over other lower theories considering in the present analysis.
- In-plane stress variation is nonlinear and has discontinuity at the layer interface.
- Increase in the volume fraction of CNT distribution in the facesheet, in general, decreases the deflection.
- The effect of temperature variation affects the stress distribution noticeable in comparison with those of the mechanical load.
- The variation in numerically computed natural frequencies through different plate theories is significant.
- For thick plate, change in the CNT distribution from UD to FGX, the higher order structural models, viz., HSDT13 and HSDT11A predicts decrease in the non-dimensionalized frequency compared to other structural models.
- The occurrence of type of flexural/extensional modes in the thickness direction depends on the location of the structures.
- The exhibition of normal stress in the thickness direction through mode shape can be demonstrated.

Acknowledgement

S Natarajan would like to acknowledge the financial support of the School of Civil and Environmental Engineering, The University of New South Wales for his research fellowship for the period September 2012 onwards.

References

References

[1] J. Whitney, Stress analysis of thick laminated composite and sandwich plates, Journal of Composite Materials 6 (1972) 426–440.

[2] A. Zenkour, A comprehensive analysis of functionally graded sandwich plates: Part 1 - deflection and stresses, International Journal of Solids and Structures 42 (2005) 5224–5242.

[3] V. Ugale, K. Singh, N. Mishra, Comparative study of carbon fabric reinforced and glass fabric reinforced thin sandwich panels under impact and static loading, Journal of Composite Materials`doi:10.1177/0021998313514874`.

[4] S. C. Tjong, Carbon nanotube reinforced composite, John-Wiley, 2009.

[5] J. Jia, J. Zhao, G. Xu, J. Di, Z. Yong, Y. Tao, C. Fang, Z. Zhang, X. Zhang, L. Zheng, Q. Li, A comparison of the mechanical properties of fibers spun from different carbon nanotubes, Carbon 49 (2011) 1333–1339.

[6] E. Thostenson, T.-W. Chou, Aligned multi-walled carbon nanotube-reinforced composites: processing and mechanical characterization, J. Phys. D: Appl. Phys 35 (2002) L77.

[7] G. Formica, W. Lacarbonara, R. Alessi, Vibrations of carbon nanotube-reinforced composites, Journal of Sound and VIbration 329 (2010) 1875–1889.

[8] P. Zhu, Z. Lei, K. Liew, Static and free vibration analyses of carbon nanotube-reinforced composite plates using finite element method with first order shear deformation plate theory, Composite Structures 94 (2012) 1450–1460.

[9] Z.-X. Wang, H.-S. Shen, Nonlinear vibration of nanotube-reinforced composite plates in thermal environment, Computational Materials Science 50 (2011) 2319–2330.

[10] A. Arani, S. Maghamikia, M. Mohammadimehr, A. Arefmanesh, Buckling analysis of laminated composite rectangular plates reinforced by SWCNTs using analytical and finite element methods, J Mech Sci Technol 25 (2011) 809–820.

[11] K. Liew, Z. Lei, J. Yu, L. Zhang, Postbuckling of carbon nanotube-reinforced functionally graded cylindrical panels under axial compression using a meshless approach, Computer Methods in Applied Mechanics and Engineering 268 (2014) 1–17.

[12] Z. Lei, K. Liew, J. Yu, Buckling analysis of functionally graded carbon nanotube-reinforced composite plates using the element free *kp*-Ritz method, Composite Structures 98 (2013) 160–168.

[13] B. S. Aragh, A. N. Barati, H. Hedayati, Eshelby-Mori-Tanaka appraoch for vivibration behavior of continuously graded carbon nanotube-reinfroced cylindrical panels, Composites Part B: Engineering 43 (2012) 1943–1954.

[14] J. Ali, K. Bhaskar, T. Varadan, A new theory for accurate thermal/mechanical flexural analysis of symmetrically laminated plates, Composite Structures 45 (1999) 227–232.

[15] M. Ganapathi, D. Makhecha, Free vibration analysis of multi-layered composite laminates based on an accurate higher-order theory, Composites Part B: engineering 32 (2001) 535–543.

[16] D. Makhecha, M. Ganapathi, B. Patel, Dynamic analysis of laminated composite plates subjected to thermal/mechanical loads using an accurate theory, Composite Structures 51 (2001) 221–236.

[17] S. Natarajan, G. Manickam, Bending and vibration of functionally graded material sandwich plates using an accurate theory, Finite Elemetns in Analysis and Design 57 (2012) 32–42.

[18] Z.-X. Wang, H.-S. Shen, Nonlinear vibration and bending of sandwich plates with nanotube-reinforced composite fnonlinear, Composites Part B: Engineering 43 (2012) 411–421.

[19] H. Murukami, Laminated composite plate theory with improved in-plane responses, Journal of Applied Mechanics 53 (1986) 661–666.

[20] J. Roderigues, C. Roque, A. Ferreira, E. Carrera, M. Cinefra, Radial basis functions-finite differences collocation and a unified formulation for bending, vibration and buckling analysis of laminated plates according to Murakami's zig-zag theory, Composite Structures 93 (2011) 1613–1620.

[21] A. Nosier, R. Kapania, J. Reddy, Free vibration analysis of laminated plates using a layerwise theory, AIAA Journal 31 (1993) 2335–2346.

[22] A. Ferreira, Analysis of composite plates using a layerwise deformation theory and multiquadratics discretization, Mech. Adv. Mater. Struct 12 (2005) 99–112.